Simultaneous Measurement of Electrical Conductivity and the Amount of Adsorbed Oxygen in Porous ZnO

Satoru FUJITSU,* Hiroshi TOYODA, Kunihito KOUMOTO, Hiroaki YANAGIDA,†
Masatoshi CHIKAZAWA,†† and Takafumi KANAZAWA††
Department of Industrial Chemistry, Faculty of Engineering, University of Tokyo, 7-3-1 Hongo, Bunkyo-ku, Tokyo 113
†Research Center for Advanced Science and Technology, University of Tokyo, 4-6-1 Komaba, Meguro-ku, Tokyo 153
††Department of Industrial Chemistry, Faculty of Technology, Tokyo Metropolitan University, 2-1-1 Fukasawa, Setagaya-ku, Tokyo 156
(Received January 11, 1988)

Changes in electrical conductivity and the amount of adsorbed oxygen in porous ZnO were measured simultaneously in the temperature range of 200—600 °C. The saturated amount of adsorbed oxygen increased initially, went through a maximum at 500 °C, and then decreased with increasing temperature. The conductivity decreased exponentially with increase in the amount of adsorbed oxygen, which indicates that the energy barrier formed due to the chemisorbed oxygen controls the total conductivity. In a high temperature region, not only the chemisorbed oxygen, but also the oxygen diffused into the grain boundaries played important roles in changing the electrical conductivity. The diffused oxygen was examined by means of a depth profile of tracer ^{18}O measured by SIMS. The formation of the energy barrier at the grain boundary was confirmed by current-voltage characteristic measurements.

Zinc oxide is an n-type semiconductor with extrinsic defects, $V_O^{\cdot}$, $V_O^{\cdot\cdot}$, $Zn_i^{\cdot}$ and/or $Zn_i^{\cdot\cdot}$.[1-4] Based on the non-stoichiometry of ZnO, the logarithm of the electrical conductivity of pure ZnO is linear with respect to that of the oxygen partial pressure with a slope of $-1/4$ or $-1/6$ depending on the ionization state of donor defects. The rate of change in electrical conductivity is determined by slow diffusion of ionic species, and so the change is too slow to be observed at low temperatures in ZnO single crystal or polycrystals with high density.

On the other hand, the change in electrical conductivity of porous ZnO is rapid and large at low temperatures (<600 °C). It is well known that the electrical conductivity of the porous ZnO depends strongly on the amount and nature of the chemisorbed oxygen.[5-10] Negatively charged chemisorbed oxygen is attained by trapping conduction electrons from the bulk of ZnO. Then, the carrier concentration decreases and the electron depletion layer to compensate the negative charge on the surface is generated, simultaneously. This depletion layer acts as the conduction barrier. In a polycrystalline sample with high density or in a single crystal, the thickness of such a layer is thin enough and its effect as the barrier can be neglected. However, considering porous ZnO in which the average neck radius to connect the grains with each other is supposed to be very small, the thickness of a depletion layer could not be neglected as shown in Fig. 1.[6] Therefore, the electrical conductivity of a porous ZnO is affected not only by the additives but also by the microstructure associated with its processing. Various electrical conductivities for porous ZnO have been reported by many researchers.[7,11-14] The decrease in the electrical conductivity caused by chemisorbed oxygen has been explained either by carrier concentration decrease due to electron trapping by chemisorbed oxygen or by surface energy barrier formation.

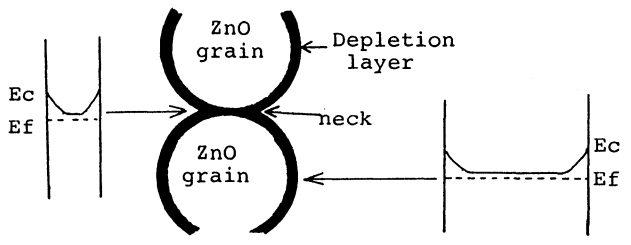

Fig. 1. Cross section of a connecting neck in a porous ZnO and energy band.

In this study, to determine the dominant mechanism for the electrical conductivity change of porous ZnO, the electrical conductivity of porous ZnO was measured as a function of the amount of adsorbed oxygen. The effect of oxygen diffused into grain boundaries was also examined by means of the depth profile of tracer (^{18}O) and the current-voltage characteristic measurements.

Experimental

(1) Sample Preparation. Nominally pure ZnO powder (99.99%, from Kojundo Chemical Lab. Co., Ltd.) was dispersed in an aqueous solution of $Al(NO_3)_3$ (99.9%, from Kanto Chemical Co., Ltd.) and dried. The resulting powder containing 0.5 mol% Al_2O_3 was calcined at 600 °C to decompose nitrate into oxide. The powder was shaped into a rectangular bar (5 by 5 by 15 mm) in a steel die (under 100 MPa pressure) and sintered at 900 °C for 1 min (S-1) or 800 °C for 1 h (S-2) in air. Aluminum oxide addition was to maintain the ZnO body porous. Of course, a trace amount of Al_2O_3 must have dissolved into the bulk ZnO promoting donor genera-

tion. To obtain a dense sample (S-3), the pressed powder was also sintered at 1300 °C for 4 h in air. The samples with the surface area of 2.1 $m^2 g^{-1}$ and 50% relative density (S-1), 3.2 $m^2 g^{-1}$ and 50% (S-2) and 95% (S-3), respectively, were obtained. SEM observation showed partial progress of sintering having occurred in the surface area of S-1 body.

(2) Electrical Conductivity and Adsorption of Oxygen. Surface area of the sample was determined by BET method at 77 K. The sample (S-1 or S-2) was enclosed in the holder illustrated in Fig. 2(b). The electrical conductivity was measured by a dc four probe method.

As the starting condition, the sample was heated at 600 °C in vacuum (10^{-4} Pa) until the conductivity reached 0.04 to 0.05 $S m^{-1}$ (about 20—25 h). At prescribed temperatures, oxygen was introduced into the holder, and the changes in the pressure and the electrical conductivity were measured simultaneously for 1 h. Change in the pressure by adsorption of oxygen was measured by using a fine vacuum gauge (BARATORON 222BA-0010 from MKS Co. Ltd.).

(3) The *I-V* Characteristic. After evacuation by the same method mentioned in (2), oxygen gas (400 Pa) was introduced into the sample holder at a fixed temperature, and after a prescribed oxidizing time the sample was quenched in liquid nitrogen. The relation between applied voltage and current was measured by a curve tracer (No. 5802 Kikusui Electronics Corp.) at room temperature.

(4) Depth Profile of Tracer ^{18}O. The enclosed sample (S-3) whose surface had been polished by diamond paste was heated at 600 °C in vacuum for 3 h, and ^{18}O (50 vol%) enriched oxygen was introduced into the sample holder at prescribed temperatures and annealed for 3 h. After annealing, the holder was quenched in liquid nitrogen.

The depth profile of tracer ^{18}O was measured by SIMS (Hitachi IMA-2A) under the so-called static SIMS condition; primary ion $^{40}Ar^+$, primary ion energy 1 keV, primary ion current 10^{-10} A, probe size 1 mm, secondary ion accelerating voltage 3 kV and residual gas pressure $<10^{-5}$ Pa.

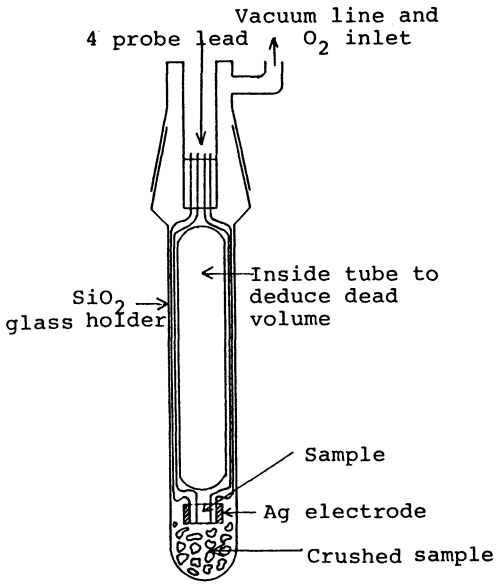

Fig. 2. Sample holder to measure the amount of adsorbed oxygen and the electrical conductivity, simultaneously.

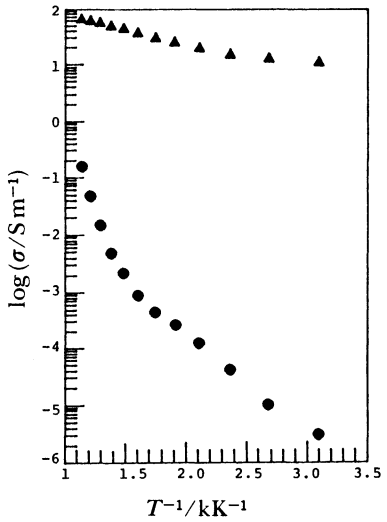

Fig. 3. Temperature dependences for a porous ZnO(S-2) in air (●) and under vacuum (▲). The electrical conductivity was measured on cooling process.

Results and Discussion

(1) Effect of Oxygen on the Electrical Conductivity of Porous ZnO. Figure 3 shows the temperature dependencies of electrical conductivity for S-2 in vacuum and in air. After annealing at 600 °C for 20 h in the respective atmosphere, the electrical conductivity was measured in the cooling process. Though the temperature dependence of electrical conductivity in vacuum was very small with an activation energy of 0.07 eV, that in air was large with an activation energy to be 2 to 3 eV.

The resulting adsorption isotherms coincided with the Langmuir type[15] in the whole temperature range from 200 to 600 °C in both samples. The saturated amount of adsorbed oxygen increased initially, went through a maximum at 500 °C and then decreased with increasing temperature in S-2. This pattern was similar to that measured by TDS (thermal desorption spectroscopy) in which the kind of chemisorbed oxygen was assumed as O^{2-},[8] while the saturated amount of adsorption decreased by repetition of the adsorption and desorption of oxygen and this effect was remarkable in S-1. This effect was explained in the following manner:[5] If high oxygen pressure causes some adsorption during sintering at high pretreatment temperature, the coulombic attraction between the adsorbed oxygen and the positively ionized defects§ may draw such defects toward the surface. Conversely, if the oxygen has been desorbed at high temperature, the adsorption centers, the defects, may diffuse away from the surface, and the number of sites for the low temperature adsorption would decrease slowly with

§ In this system, zinc atoms at interstitial sites, oxygen vacancies and substituted Al are the candidates for these defects.

time. Though the saturated amount of adsorption slightly depended on the order of measurement, the tendency of the temperature dependence of the saturated amount for S-1 with a low surface area corresponded to that measured by TDS.

Electrical conductivity decreased with increase in the amount of adsorbed oxygen in the whole temperature range as shown in Fig. 4. If the decrease in electrical conductivity resulted from the decrease in the total carrier concentration, the conductivity should have decreased linearly with increase in the amount of adsorbed oxygen which behaves as the electron trap. So, this model could not account for the change in the conductivity.

The effect of oxidation and reduction in the bulk should be also considered. The dependence of electrical conductivity on oxygen partial pressure was larger than expected from the change in nonstoichiometric composition by atmosphere. And the conductivity did not change above the pressure to attain saturation of adsorption which is approximately 1000 Pa at 600 °C. From these experimental results it is judged that oxidation and reduction in the bulk would have a the minor effect on changing the electrical conductivity in the present temperature and pressure regions.

The assumption that the energy barrier whose height increases with increase in the amount of adsorbed oxygen controls the total conductivity, could explain this result. Considering that the carrier mobility is constant throughout the sample, the electrical conductivity of a semiconductive material depends on the energy difference between the bottom of the conduction band (E_c) and the Fermi level (E_f) as $\sigma \propto \exp(-(E_c-E_f)/kT)$. The difference ($E_c-E_f$) is very small, about several hundredths of an electron volt as appeared in the temperature dependence measured in vacuum (Fig. 3). The presence of energy barrier makes this energy difference to be large as shown in Fig. 1. If

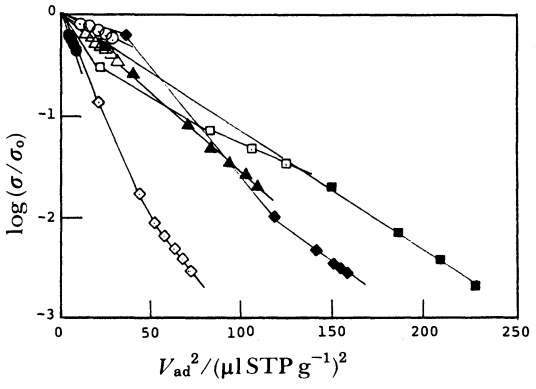

Fig. 4. The change of electrical conductivity against the amount of adsorbed oxygen: $\log(\sigma/\sigma_o)-V_{ad}^2$ where σ_o is the electrical conductivity in vacuum. Sample S-1; ●: 300 °C, ▲: 400 °C, ■: 500 °C, ◆: 600 °C. Sample S-2; ○: 300 °C, △: 400 °C, □: 500 °C, ◇: 600 °C.

the chemisorbed oxygen makes an acceptor type trap level on the surface of ZnO, the resulting energy barrier to compensate the excess charge is generated. The height of such a surface energy barrier (ϕ_s) is estimated as[5,16]

$$\phi_s = \frac{2eN_{ss}^2}{\varepsilon\varepsilon_o N_d} \quad (1)$$

where N_{ss} the trap state density which is proportional to the amount of adsorbed oxygen, N_d the donor density and the other symbols have their usual meanings. When N_{ss} is large, the change in the height, $\Delta\phi_s$, is approximated to be proportional to the change in N_{ss}. The effective thickness of such a barrier is so small that this effect is negligible in single crystal or polycrystal with high density. While this barrier plays an important role to decrease the conductivity in the case of porous body where a narrow neck connects the grains with each other. When this barrier is formed into an interior of the narrow neck region, the total conductivity should be controlled by such necks as $\sigma \propto \exp(-(E_{cv}- E_f+\phi)/kT)$ where E_{cv} is the bottom of the conduction band in vacuum and ϕ is the effective barrier height. Though the height of energy barrier at the surface is estimated by Eq. 1., the effective height is determined by the lowest energy barrier at the center of the cross section of the neck.

If the conductivity measured in this experiment was controlled by the mechanism discussed above, $\log(\sigma/\sigma_o)$ in Fig. 4 equals to ϕ/kT and the decrease in conductivity by two orders of magnitude corresponds to the generation of the energy barrier with an effective height to be 0.3 eV at 500 °C. The ϕ/kT increased linearly with increase in the amount of adsorbed oxygen at 600 °C or its square at 300—500 °C. This dependence agrees with the rule of generation of the surface energy barrier by the surface state of acceptor type. The effective height of the energy barrier might reflect the height of the surface energy barrier. The right end plot of each measurement almost agreed with the saturation of the change in the electrical conductivity and the adsorption of oxygen. Though the change in electrical conductivity depended on the amount of adsorbed oxygen in S-2 with a large surface area, that in S-1 with a smaller surface area showed a larger change in electrical conductivity at 600 °C where the amount of adsorption is smaller than at 500 °C. It is peculiar that a similar change in the electrical conductivity was observed in S-1 and S-2 at 600 °C. These results suggest that another mechanism is operative to change the electrical conductivity. When the surface energy barrier controls the total conductivity, the grains should be connected with each other by a small neck with the width to be comparable to the thickness of the depletion layer. The thickness of this layer is approximately by the Debye length.[7] The samples of this experiment contain Al_2O_3 as a promoter of donor

generation. Though the exact solubility limit of Al_2O_3 into ZnO has not been determined, the thickness is estimated to be below 10 nm by the assumption that 100 ppm of Al_2O_3 could dissolve into ZnO.

Because of the complicated microstructure, the precise neck radius could not be determined. Two kinds of samples, S-1 and S-2, have almost the same relative density of 50% and the average grain size of 0.5 μm. From the viewpoint of surface area, it is supposed that the neck radius of S-2 might be larger than that of S-1. Since the current flows through the wide neck which is difficult to form the barrier in its interior, the effective neck radius might have been enhanced by the partial progress of sintering in S-1. Considering that the neck radius of S-1 is larger than the thickness of the surface energy barrier, the smaller change in the electrical conductivity in S-1 by the oxygen chemisorption could be explained, i.e., the formation of the energy barrier is imperfect in S-1.

On the other hand, the anomalous change in the conductivity at 600 °C has not been clarified yet. Recognizing the neck as the grain boundary and assuming that the selective oxidation of the grain boundary by the rapid oxygen diffusion into such an area occurs, the energy barrier should be generated at the grain boundary and considerably change the electrical conductivity even in a sample with wide neck. Though the definite model to explain the formation of the barrier by the selective oxidation of the grain boundary could not be determined by this experiment, two models have been proposed for ZnO varistor: one is the formation of stoichiometric ZnO near the grain boundary regions,[17] and the other is the generation of acceptor states due to oxygen chemisorption along the grain boundaries.[18]

(2) The Energy Barrier along the Grain Boundary. If the energy barrier along the grain boundary is formed in ZnO, the non-ohmic behavior of resistivity should be observed like a varistor.[19,20] As reported in our previous paper, the non-ohmic property was observed in the porous ZnO.[21] From the proposed tunnel theory,[20] the non-ohmic coefficient, α, in the expression $I=(V/C)^{\alpha}$, where I is the current, V the applied voltage and C a constant, can be written as

$$\alpha = \frac{4}{3}(m\varepsilon_s)^{1/2}\frac{V}{hN_d^{1/2}(1+V/\phi)^{3/2}} \qquad (2)$$

where ϕ is the barrier height, N_d the donor density, V the applied voltage, and the other symbols have their usual meanings. Though it is not yet recognized which mechanism controls the non-ohmic characteristic in this experiment, the higher the barrier is, the larger α becomes in any model if the donor density is constant. As shown in Fig. 5,[18] the non-ohmic coefficient, α, increased with an increase in the oxidizing period, and α larger at 600 °C where the oxygen diffusion might be effective to generate the energy barrier than at 500 °C where the amount of adsorption was larger than that at 600 °C in S-1, while in the case of S-2 the maximum non-ohmic coefficient, α, was attained by the oxidation within several minutes. Therefore, the high energy barrier along the grain boundary is also formed by oxygen diffusion at 600 °C in even a wide neck. The deterioration of the characteristic for the sample oxidized for 24 h is explained by the diffusion into the bulk; i.e., the difference in chemical potential between the bulk and grain boundary might decrease.

(3) Oxygen on the Surface and in the Bulk. In the previous sections, the phenomena which could not be explained by the adsorption of oxygen were discussed on the assumption that the energy barrier along the grain boundary was formed by the rapid diffusion of oxygen into the grain boundary. To confirm the

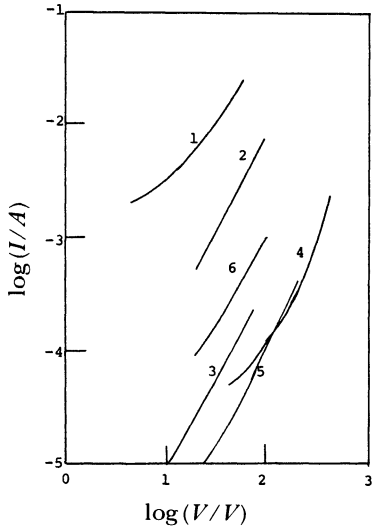

Fig. 5. I–V relation for porous ZnO under various oxidation conditions; (1) 1 min at 600 °C (α=1.31), (2) 3 min at 600 °C (1.68), (3) 10 min at 600 °C (2.28), (4) 1 h at 600 °C (2.93), (5) 24 h at 600 °C (2.44), and (6) 1 h at 500 °C (1.91).

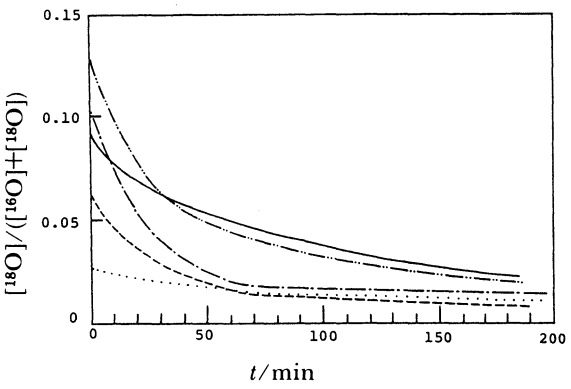

Fig. 6. The depth profile of tracer (^{18}O) in dense ZnO. --------: 200 °C, ----: 300 °C, -·-·-: 400 °C, -···-···-: 500 °C. ——: 600 °C.

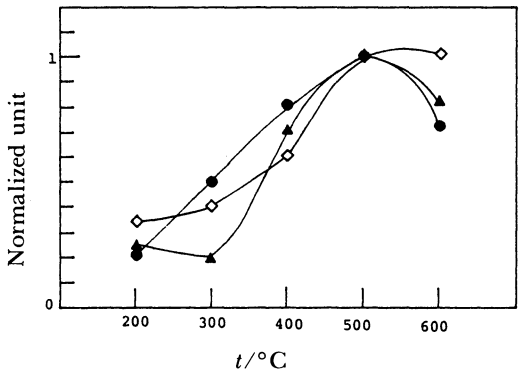

Fig. 7. The saturated amount of adsorbed oxygen, the tracer concentration at surface and the integrated concentration calculated from Fig. 5. The values were normalized under the condition as $V/V_{500°C}$. ●: from Langmuir's method ($V_a/V_{a500°C}$), ▲: Surface concentration ($V_s/V_{s500°C}$), ◇: Integrated concentration ($V_i/V_{i500°C}$).

validity of this assumption, the oxygen diffusion into the grain boundary should be examined.

The depth profiles of tracer ^{18}O in ZnO annealed at prescribed temperatures are shown in Fig. 6. In all measurements, the strengths of the primary beam of SIMS were weak and constant. Figure 6 shows the atomic fraction of ^{18}O against the measuring period. The measured fraction at the beginning might be strongly affected by the chemisorbed oxygen and that after long measuring period might indicate the effect of the penetration of oxygen into the interior of the sample. Though this time corresponds to the depth of etched crater, the depth was too small to be measured precisely. Hence, the correct diffusion coefficient could be not estimated.

In the temperature region 200—500 °C, the concentration of tracer increased with increasing temperature. At 600 °C, the concentration of tracer at the surface was smaller than that at 500 °C, but on the other hand, that in the interior was larger than that at 500 °C. The saturated amount of adsorption measured by Langmuir's method (V_a) for S-1, the tracer concentration at the surface (V_s) and the integrated concentration calculated from Fig. 6 in the time range 0 to 3 h (V_i) are shown in Fig. 7. Each plot was normalized to the values obtained at 500 °C as $V/V_{500°C}$. Though the temperature dependencies of V_a and V_s were similar in the whole temperature range, the V_i at 600 °C was larger than that at 500 °C. From Fig. 7, V_s reflects the amount of adsorbed oxygen. The integrated value (V_i) involved not only the enrichment of the tracer at the surface but also that in the interior.

The observation of the enrichment of the tracer in the interior of the sample indicated that the diffusion of oxygen effectively occurred at 600 °C. It is well known that the oxygen diffusion is accelerated along grain boundaries. The oxygen transport by diffusion is higher at higher temperatures and the difference in the diffusion rate between the grain and grain boundary is large at low temperatures due to the difference in its activation energy. The rapid diffusion along the grain boundary was observed even at 1000 °C.[22,23] Therefore, it would be reasonable to consider that the grain boundary is oxidized selectively at 600 °C by the rapid grain boundary diffusion, and this area might become the energy barrier for electron transport.

The authors wish to thank Dr.Shunichi Hishita of National Institute for Research in Inorganic Materials for analysis of the depth profile by using SIMS and helpful discussion. They also wish to thank Mr. Shigeru Ando of Ando Glass Blowing Technology Ltd. for his excellent technique for glass blowing. This work was partially supported by a Grant-in-Aid for Scientific Research from the Japanese Ministry of Education, Science and Culture (No. 60550543).

References

1) M. H. Sukkar and H. L. Tuller, "Additives and Interface in Electronic Ceramics," ed by M. F. Yan and A. H. Heuer, The American Ceramics Society, Columbus (1983), pp. 71—90.
2) K. I. Hagemark and L. C. Chocka, *J. Solid State Chem.*, **15**, 261 (1975).
3) K. I. Hagemark, *J. Solid State Chem.*, **16**, 292 (1976).
4) K. Koumoto and H. Yanagida, *Ceram. Jpn.*, **18**, 927 (1983).
5) S. R. Morrison, *Adv. Catal.*, **7**, 259 (1955).
6) N. M. Beekmans, *J. Chem. Soc., Faraday Trans. 1*, **74**, 31 (1978).
7) M. Takata and H. Yanagida, *Yogyo Kyokaishi*, **87**, 19 (1979).
8) W. Gopel, *J. Vac. Sci. Technol.*, **15**, 1298 (1978).
9) N. Miura, O. Nakagawa, N. Yamazoe, and T. Seiyama, *Denki Kagaku*, **49**, 367 (1981).
10) H. Chon and J. Pajares, *J. Catal.*, **14**, 257 (1969).
11) P. H. Miller, *Phys. Rev.*, **60**, 890 (1941).
12) M. Takata, D. Tsubone, and H. Ynagida, *J. Am. Ceram. Soc.*, **59**, 4 (1976).
13) K. Intemann and F. Stockmenn, *Z. Physic*, **131**, 10 (1950).
14) P. Chandra, V. B. Tare, and A. P. B. Sinha, *Indian J. Pure Appl. Phys.*, **5**, 313 (1967).
15) I. Langmuir, *J. Am. Chem. Soc.*, **40**, 1361 (1918).
16) R. H. Kingston and S. F. Neustadter, *J. Appl. Phys.*, **26**, 718 (1955).
17) R. Einginger, *Appl. Surf. Sci.*, **3**, 390 (1979).
18) K. Tsuda and K. Mukae, "High Tech Ceramics," ed by P. Vincentini, Elsevier (1987), p. 1781.
19) M. Matsuoka, *Jpn. J. Appl. Phys.*, **10**, 736 (1971).
20) K. Mukae, K. Tsuda, and I. Nagasawa, *Jpn. J. Appl. Phys.*, **16**, 1361 (1977).
21) S. Fujitsu, H. Toyoda, and H. Yanagida, *J. Am. Ceram. Soc.*, **70**, C71 (1987).
22) S. Shirasaki, Y. Moriyoshi, H. Yamamura, H. Haneda, K. kakegawa, K. Manabe, and M. Ogawa, *Zairyo*, **31**, 850 (1982).
23) W. J. Moore and E. L. William, *Disc. Faraday Soc.*, **28**, 86 (1959).